

## Search for Charged Strange Quark Matter Produced in 11.5A GeV/c Au + Pb Collisions

T. A. Armstrong,<sup>7</sup> K. N. Barish,<sup>12,\*</sup> M. J. Bennett,<sup>12</sup> S. J. Bennett,<sup>11</sup> A. Chikanian,<sup>12</sup> S. D. Coe,<sup>12</sup> T. M. Cormier,<sup>11</sup> R. Davies,<sup>8</sup> G. De Cataldo,<sup>1</sup> P. Dee,<sup>11,†</sup> G. E. Diebold,<sup>12</sup> C. B. Dover,<sup>2,‡</sup> P. Fachini,<sup>11</sup> L. E. Finch,<sup>12</sup> N. K. George,<sup>12</sup> N. Giglietto,<sup>1</sup> S. V. Greene,<sup>10</sup> P. Haridas,<sup>6</sup> J. C. Hill,<sup>4</sup> A. S. Hirsch,<sup>8</sup> R. A. Hoversten,<sup>4</sup> H. Z. Huang,<sup>3,§</sup> B. Kim,<sup>11</sup> B. S. Kumar,<sup>12,||</sup> T. Lainis,<sup>9</sup> J. G. Lajoie,<sup>12</sup> R. A. Lewis,<sup>7</sup> Q. Li,<sup>11</sup> B. Libby,<sup>4,¶</sup> R. D. Majka,<sup>12</sup> M. G. Munhoz,<sup>11</sup> J. L. Nagle,<sup>12,\*\*</sup> I. A. Pless,<sup>6</sup> J. K. Pope,<sup>12</sup> N. T. Porile,<sup>8</sup> C. A. Pruneau,<sup>11</sup> M. S. Z. Rabin,<sup>5</sup> A. Raino,<sup>1</sup> J. D. Reid,<sup>7,††</sup> A. Rimai,<sup>8,‡‡</sup> F. S. Rotondo,<sup>12</sup> J. Sandweiss,<sup>12</sup> R. P. Scharenberg,<sup>8</sup> A. J. Slaughter,<sup>12</sup> G. A. Smith,<sup>7</sup> P. Spinelli,<sup>1</sup> B. K. Srivastava,<sup>8</sup> M. L. Tincknell,<sup>8</sup> W. S. Toothacker,<sup>7</sup> G. Van Buren,<sup>6</sup> W. K. Wilson,<sup>11</sup> F. K. Wohn,<sup>4</sup> E. J. Wolin,<sup>12,§§</sup> Z. Xu,<sup>12</sup> and K. Zhao<sup>11</sup>

(The E864 Collaboration)

<sup>1</sup>University of Bari/INFN, Bari, Italy

<sup>2</sup>Brookhaven National Laboratory, Upton, New York 11973

<sup>3</sup>University of California at Los Angeles, Los Angeles, California 90095

<sup>4</sup>Iowa State University, Ames, Iowa 50011

<sup>5</sup>University of Massachusetts, Amherst, Massachusetts 01003

<sup>6</sup>Massachusetts Institute of Technology, Cambridge, Massachusetts 02139

<sup>7</sup>Pennsylvania State University, University Park, Pennsylvania 16802

<sup>8</sup>Purdue University, West Lafayette, Indiana 47907

<sup>9</sup>United States Military Academy, West Point, New York 10996

<sup>10</sup>Vanderbilt University, Nashville, Tennessee 37235

<sup>11</sup>Wayne State University, Detroit, Michigan 48201

<sup>12</sup>Yale University, New Haven, Connecticut 06520

(Received 21 November 1996; revised manuscript received 5 June 1997)

We present results of a search for strange quark matter (strangelets) in 11.5A GeV/c Au + Pb collisions from the 1994 and 1995 runs of experiment E864 at Brookhaven's Alternating Gradient Synchrotron. We observe no strangelet candidates and set a 90% confidence level upper limit of approximately  $3 \times 10^{-8}$  per 10% central interaction for the production of  $|Z| = 1$  and  $|Z| = 2$  strangelets over a large mass range and with metastable lifetimes of about 50 ns or more. These results place constraints primarily on quark-gluon plasma based production models for strangelets. [S0031-9007(97)04465-7]

PACS numbers: 25.75.-q

Color-singlet hadrons with baryon number  $A > 1$ , called *quark matter*, are allowed in the standard model but have never been observed by experiment. All the quarks within this type of state would be free within the hadron's boundary, and would not be subject to grouping into the familiar  $A = 1$  baryons. In this way it is different from a nuclear state, which is a conglomerate of  $A = 1$  baryons.

Quark matter states containing up and down quarks, if they exist, are less stable (more massive) than nuclei with the same baryon number and charge, since nuclei do not decay into quark matter. This is presently understood to be a consequence of the relatively large Fermi energy of two-flavor quark matter. However, additional quark flavors could possibly reduce the Fermi energy of quark matter [1]. Hence strange quark matter (SQM), which would contain strange quarks in addition to up and down quarks, might be more stable than nonstrange quark matter with the same  $A$ , despite the mass of the strange quark. Other quarks are usually not considered since they are

much more massive than the strange quark, and thus are not expected to enhance stability. Since SQM systems are expected to contain approximately equal numbers of up, down, and strange quarks (with charges  $+2/3e$ ,  $-1/3e$ , and  $-1/3e$ , respectively), they would have lower charge-to-mass ratios than nearly all ordinary nuclei. This property is the basis for all current SQM searches at heavy ion accelerators.

Studies have used quantum chromodynamics (QCD) and the MIT bag model of hadrons [2] to treat SQM quantitatively [3–5]. All of the theories contain the feature that SQM systems become more stable as  $A$  increases, due to the small total charge of SQM as well as bag model effects. For sufficiently large  $A$  ( $A \sim 100$  to  $A \sim 10\,000$ , depending on the parameters assumed), SQM may be absolutely stable [6]. For smaller,  $A$ , SQM may be metastable, that is stable against strong decays but subject to weak decays with lifetimes in the range  $10^{-4}$  to  $10^{-10}$  sec [3,7,8]. SQM systems with  $A \leq 100$ , which might be produced in high energy heavy ion collisions,

are predicted to be metastable for a wide range of SQM properties and bag model parameters [8]. These smaller systems are commonly called *strangelets*.

Three types of production models have been applied to strangelet production in nucleus-nucleus collisions. In the first type, called *coalescence models*, a group of known  $A = 1$  particles are made which, in sum, contain the same quantum numbers (baryon number, strangeness, and charge) as a viable strangelet, and then these ingredients fuse to form a strangelet [9]. A second type of production, called *thermal models*, assume further that chemical and thermal equilibrium are achieved prior to final particle production [10]. Coalescence and thermal models usually predict lower strangelet cross sections than the last type of model, in which an intermediate quark-gluon plasma (QGP) state is formed after the initial nucleus-nucleus collision, and the QGP loses energy in a way that possibly favors strangelet production. Kapusta *et al.* have estimated that a QGP would be produced between 0.1% and 1% of central (small impact parameter) Au + Au collisions at AGS energies [11]. Greiner *et al.* have suggested that, for a wide range of assumed properties of the QGP, nearly every such QGP state would evolve into a strangelet by a strangeness distillation mechanism if strangelets are stable or metastable [12]. Other distillation estimates predict a wide range of production levels [13,14]. Thus strangelet production could be as high at  $10^{-4}$  to  $10^{-3}$  per central Au + Au collision, well within the sensitivity to be presented here. Note also that a strangelet produced by the strangeness distillation of a QGP could have approximately the same  $A$  as the QGP itself, since the QGP would largely lose energy by meson—not baryon—emission. Hence it is of considerable interest for experiments to remain sensitive to a large mass range.

Early strangelet searches in Si + Cu collisions [15], Si + Au [16], and in S + W collisions [17] yielded null results. More recently, experiments utilizing Au beams at Brookhaven National Laboratory (BNL) [18,19] and Pb beams at CERN [20] saw no evidence for strangelet production, despite the increased production potential of these heavier beams. The experiments were sensitive to particles with proper lifetimes of about 50 ns or more, depending on the experiment. All these experiments, with the exception of the one described in Ref. [15], used focusing spectrometers which, at a given magnetic field setting, have good acceptance for a fixed rigidity  $R = p/Z$ , where  $p$  is the momentum and  $Z$  is the charge of the produced particle. The production limits obtained using these spectrometers are strongly dependent upon the production model assumed for high mass particles such as strangelets. In this paper we show the results of an open geometry spectrometer experiment (containing dipole-type magnets only) whose sensitivity is less subject to the shape of a particle's differential cross section. We examine the mass range  $m \geq 5 \text{ GeV}/c^2$  and  $m \geq 6 \text{ GeV}/c^2$  for  $Z = +1$  and  $Z = +2$ , respectively, and  $m \geq 5 \text{ GeV}/c^2$  for  $Z = -1$  and  $Z = -2$ . Our

sensitivities slowly fall off for very high masses (e.g., our acceptance falls by a factor of 3 for a mass  $500 \text{ GeV}/c^2$  object compared to a mass  $50 \text{ GeV}/c^2$  object for the production models discussed below). We are sensitive to particles with proper lifetimes greater than about 50 ns.

A schematic diagram of the E864 spectrometer is shown in Fig. 1. An  $11.5 \text{ GeV}/c$  per nucleon Au beam enters from the left through a quartz Cerenkov beam counter and veto counters [21], and is incident on a Pb target. A segmented scintillator multiplicity counter measures an interaction's products within an angular range of  $16.6^\circ$  to  $45^\circ$  with respect to the incident beam, providing a rough measure of the impact parameter, or centrality, of the reaction [21]. For this analysis, we require the multiplicity counter's pulse height to exceed a threshold such that 10% of the total Au + Pb cross section is accepted. This multiplicity trigger thus accepts roughly the 10% most central (smallest impact parameter) events (see [21,22] for further details). Interaction products which are within the experimental acceptance pass through two dipole magnets labeled M1 and M2, and proceed through downstream detectors. Three segmented planes of scintillation counters (hodoscopes) labeled H1, H2, and H3, each contain 206 vertical scintillator slats viewed with photomultiplier tubes located at the top and bottom of the slats. Each photomultiplier signal is digitized for both pulse height and time information. Three arrays of 4 mm diameter straw tubes labeled S1, S2, and S3 provide high resolution position measurements. The straw signals are digitized in a latch system. Each array includes three planes of doublet layers. Two of the layers are inclined at  $\pm 20^\circ$  to the vertical, so that they provide a measurement of the vertical as well as the horizontal coordinate. S1 was not used in this analysis. A lead/scintillating fiber hadronic calorimeter labeled CAL terminates the apparatus [23]. It consists of 754 towers, each of which is read out by a photomultiplier tube. These photomultiplier signals are digitized for both pulse height and time information, and thus provide energy and time-of-flight

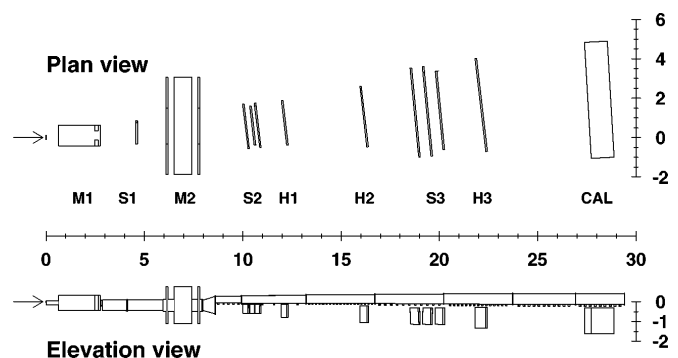


FIG. 1. Schematic views of the E864 spectrometer. In the plan view, the downstream vacuum chamber is not shown. M1 and M2 are dipole analyzing magnets, S2 and S3 are straw tube arrays. H1, H2, and H3 are scintillator hodoscopes, and CAL is a hadronic calorimeter. The horizontal and vertical scales are in meters.

measurements. The calorimeter is also used to form a high-level trigger that correlates the energy and time-of-flight signature of showers on a tower-by-tower basis, and is set to identify particles of high mass. This trigger, called the *late-energy trigger* or LET, provides the experiment with a rejection factor of about 50 in 10% central interactions. A paper on the E864 apparatus is forthcoming [24].

The charge ( $Z$ ) of a particle that traverses the spectrometer is measured using pulse height information from the three hodoscope walls. Its rigidity ( $R$ ) is derived from the target position and downstream slope and position of the particle's track in the spectrometer's magnetic bend plane, as measured by the straw tube and hodoscope detectors. The particle's velocity is measured using timing information from the hodoscopes, and this gives the relativistic quantities  $\beta$  and  $\gamma$ . The particle's mass ( $m$ ) is then reconstructed as  $m = \frac{R}{\gamma\beta}Z$ . The calorimeter's time and energy information was used to confirm the above measurements or reject potential backgrounds. This analysis was confined to a rapidity range about 1.3 units wide near the center-of-mass rapidity value of 1.6, as we expect strangelet production to be peaked in this region.

The strangelet analysis presented here uses over  $120 \times 10^6$  10% central Au + Pb events taken from different magnetic field settings during two separate running periods. A preliminary strangelet search for positively charged strangelets was performed in 1994 with a partially completed apparatus. Analysis methods were developed largely using data from this first run, and the experiment's capabilities were learned, especially concerning the dominant background process in our spectrometer [22,25,26]. Our spectrometer was completed and optimized for both positively and negatively charged strangelet states in our 1995 run [27,28], and these searches achieved excellent sensitivity due to the high-rejection LET trigger.

We observe clear peaks in our mass distributions for  $Z = 1$  objects such as  $p$ ,  $d$ ,  $t$ ,  $K^-$ , and  $\bar{p}$ , and  $Z = 2$  objects such as  ${}^3\text{He}$ ,  ${}^4\text{He}$ , and  ${}^6\text{He}$ , including over 50  ${}^6\text{He}$  nuclei measured within  $\pm 0.6$  units of midrapidity. The mass resolutions are as expected considering the detector resolutions and multiple scattering in the spectrometer.

We observe no strangelet candidates in our 1995 data with  $m > 5 \text{ GeV}/c^2$  for  $Z = +1$ ,  $Z = -1$ , and  $Z = -2$  systems, and we observe no candidates with  $m > 6 \text{ GeV}/c^2$  for  $Z = +2$  systems.

In order to set limits on strangelet production, we compute the following expression for the number of candidates observed:

$$N_{\text{obs}} = \frac{I_{\text{central}}}{\sigma_{\text{central}}} \int \epsilon(y, p_t) \frac{d^2\sigma}{dy dp_t} dy dp_t, \quad (1)$$

where  $N_{\text{obs}}$  is the number of strangelets observed,  $I_{\text{central}}$  is the number of central interactions examined,  $\sigma_{\text{central}}$  is the cross section for 10% central Au + Pb interactions (10% of the total Au + Pb cross section),  $\epsilon(y, p_t)$  is

the efficiency for detecting a strangelet as a function of  $y$  and transverse momentum ( $p_t$ ), and  $d^2\sigma/dy dp_t$  is the strangelet differential cross section. We take the differential cross section to be separable in  $y$  and  $p_t$ ,

$$\frac{d^2\sigma}{dy dp_t} = \sigma_s \left[ \left( \frac{2}{\langle p_t \rangle} \right)^2 p_t e^{-2p_t/\langle p_t \rangle} \right] \times \left[ \frac{1}{\sqrt{2\pi} w} e^{-(y-y_{cm})^2/2w^2} \right], \quad (2)$$

where  $\sigma_s$  is the total strangelet cross section in central collisions,  $y_{cm}$  is the center-of-mass rapidity, and  $w$  is the rms width (standard deviation) of the rapidity distribution of the strangelet. We take  $w = 0.5$  and  $\langle p_t \rangle = 0.6\sqrt{A} \text{ GeV}/c$ .

Since  $N_{\text{obs}} = 0$  in our analysis, we can say from Poisson statistics that there is a 90% chance that  $N_{\text{obs}} < 2.3$ . By inverting Eq. (1), we obtain a 90% confidence level (90% C.L.) upper limit on strangelet production per central interaction. Figure 2 shows E864's 90% C.L. limits for positive and negative strangelets with lifetimes greater than 50 ns produced in 11.5 GeV/c Au + Pb interactions. The 4 curves which display our 1995 results in Fig. 2 begin well above the mass distributions of known particles reconstructed in our data. These starting values are 4.7, 4.7, 5.6, and 7.5 GeV/c<sup>2</sup> for  $Z = -2, -1, +1, +2$ , respectively. Also shown in the figure are our 1994 results, which are more fully described in Refs. [22,26].

E864's upper limits are nearly flat as a function of mass, owing to the large acceptance of the spectrometer. These limits are only mildly sensitive to changes in Eq. (2) for the same reason. For example, if the rapidity

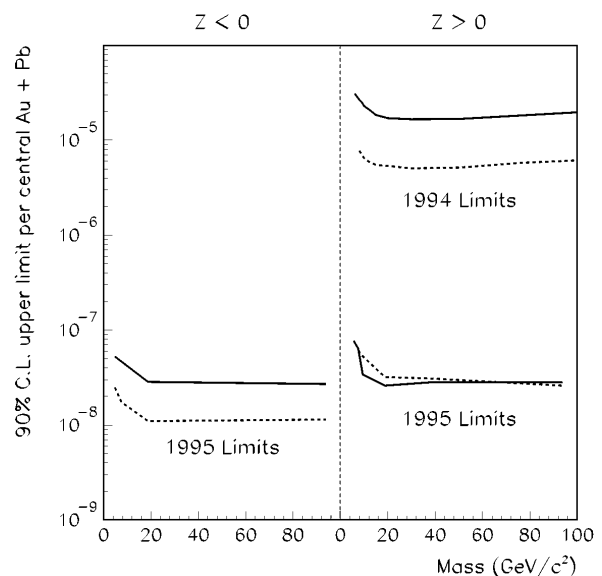


FIG. 2. 90% confidence level limits for  $|Z| = 1$  and  $|Z| = 2$  strangelet production in 10% central Au + Pb collisions, for strangelets with lifetimes greater than 50 ns. The solid lines correspond to  $|Z| = 1$ , while the dashed lines correspond to  $|Z| = 2$ .

width of strangelet production were taken to be  $w = 0.5/\sqrt{A}$ , the E864 curves in Fig. 2 would be lower (give better limits) by less than a factor of 2.

The production of SQM depends on both its properties and cross section for its production in heavy ion interactions. If we assume that SQM production rates are larger than our sensitivities, then we are either constraining SQM lifetimes to  $\tau \ll 50$  ns, or bag model parameters as applied to SQM (so that SQM is either unstable for all  $A$  or metastable only when  $A \gg 100$ ). According to Refs. [7,8], a wide range of strangelets are expected to undergo semileptonic and radiative decays only [8] which would have relative long lifetimes, so we may be placing constraints on bag model parameters. While intriguing, this possibility must remain unanswered until the issues of strangelet production are fully addressed.

The sensitivity of this analysis is comparable to the coalescence production levels for low-mass strangelets. For example, a strangelet with  $A = 7$  and strangeness  $S = -4$  could be produced at approximately the same level as the hypernucleus  $\Xi_{\Lambda\Lambda}^0 \text{He}$ , since these states have the same quantum numbers  $A$  and  $S$ . Reference [9] estimates  $\Xi_{\Lambda\Lambda}^0 \text{He}$  will be produced between  $3 \times 10^{-8}$  and  $7.2 \times 10^{-8}$  per central Au + Au collision at the AGS, while our sensitivity for this state is about  $6 \times 10^{-8}$  per central Au + Pb collision. It appears, however, that the model in Ref. [9] is optimistic, since a preliminary analysis of data shows that the model overpredicts light nucleus production [29]. Thermal models would predict production below our sensitivity for low-mass strangelets. For example, the  $\Xi_{\Lambda\Lambda}^0 \text{He}$  rate is computed to be  $\sim 2 \times 10^{-10}$  in Au + Au collisions in Ref. [10]. For larger mass strangelets, both coalescence and thermal models predict production below our sensitivity. Our limits do constrain the sequence of QGP production [11] followed by QGP decay into a strangelet [12]. For a  $10 \leq m \leq 100$  GeV/ $c^2$  strangelet with  $|Z| = 1$  or  $|Z| = 2$  and lifetime above 50 ns, our data approximately restrict these processes (cf. with Fig. 2) at the 90% confidence level as follows:

$$\begin{aligned} B(\text{Au} + \text{Pb} \rightarrow \text{QGP}) \times B(\text{QGP} \rightarrow \text{strangelet}) \\ \lesssim 3 \times 10^{-8}, \end{aligned} \quad (3)$$

where  $B(\text{Au} + \text{Pb} \rightarrow \text{QGP})$  is the probability for a 10% central Au + Pb collision at 11.5 GeV/ $c$  to produce a QGP, and  $B(\text{QGP} \rightarrow \text{strangelet})$  is the probability of the QGP to decay into the strangelet in question. Some QGP production estimates for strangelets are largely ruled out by our results [13], while others are being challenged. For example, Ref. [14] predicts a strangelet with  $A = 10$ ,  $Z = 2$  to be produced  $7.5 \times 10^{-8}$  per central Si + Au interaction (with expected higher yields in Au + Pb interactions), which is above our limit of  $5.3 \times 10^{-8}$  per central Au + Pb interaction for the same strangelet.

In summary, we have found no evidence for strangelet production in 11.5 GeV/ $c$  per nucleon Au + Pb collisions,

and set a 90% confidence level upper limit of about  $3 \times 10^{-8}$  per 10% central Au + Pb interaction for the production of  $Z = |1|$  and  $Z = |2|$  strangelets over a wide mass range and with lifetimes about 50 ns or more. This represents the highest sensitivity strangelet search yet achieved in a heavy ion experiment at AGS energies.

We gratefully acknowledge the efforts of the BNL AGS staff. This work was supported by grants from the U.S. Department of Energy's High Energy and Nuclear Physics Divisions, the U.S. National Science Foundation, and the Istituto Nazionale di Fisica Nucleare of Italy.

\*Present address: University of California at Los Angeles, Los Angeles, CA 90095.

†Present address: Positron Imaging Centre, Birmingham University, Birmingham, England.

‡Deceased.

§Previously at Purdue University.

||Present address: McKinsey & Co., New York, NY 10022.

¶Present address: Department of Radiation Oncology, Medical College of Virginia, Richmond, VA 23298.

\*\*Present address: Columbia University, Nevis Laboratory, Irvington, NY 10533.

††Present address: Vanderbilt University, Nashville, TN 37235.

‡‡Present address: Institut de Physique Nucléaire, 91406 Orsay Cedex, France.

§§Present address: College of William and Mary, Williamsburg, VA 23185.

- [1] In the limit of a simple relativistic Fermi gas of massless quarks, the energy of quark matter is proportional to  $n_f^{-1/3}$ , where  $n_f$  is the number of quark flavors in the system.
- [2] A. Chodos *et al.*, Phys. Rev. D **9**, 3471 (1974).
- [3] S. Chin and A. Kerman, Phys. Rev. Lett. **43**, 1292 (1979).
- [4] E. Farhi and R. Jaffe, Phys. Rev. D **30**, 2379 (1984).
- [5] E. Gilson and R. Jaffe, Phys. Rev. Lett. **71**, 332 (1993).
- [6] E. Witten, Phys. Rev. D **30**, 272 (1984).
- [7] M. S. Berger and R. L. Jaffe, Phys. Rev. C **35**, 213 (1987).
- [8] G. L. Shaw *et al.*, Nature (London) **337**, 436 (1989).
- [9] A. Baltz *et al.*, Phys. Lett. B **325**, 7 (1994).
- [10] P. Braun-Munzinger and J. Stachel, J. Phys. G **21**, L17 (1995).
- [11] J. Kapusta *et al.*, Phys. Rev. C **51**, 901 (1995); J. Kapusta and A. Vischer, Phys. Rev. C **52**, 2725 (1995).
- [12] C. Greiner *et al.*, Phys. Rev. Lett. **58**, 1825 (1987); C. Greiner and H. Stöcker, Phys. Rev. D **44**, 3517 (1991).
- [13] H. C. Liu and G. L. Shaw, Phys. Rev. D **30**, 1137 (1984).
- [14] H. Crawford *et al.*, Phys. Rev. D **45**, 857 (1992).
- [15] J. Barrette *et al.*, Phys. Lett. B **252**, 550 (1990).
- [16] A. Aoki *et al.*, Phys. Rev. Lett. **69**, 2345 (1992).
- [17] K. Borer *et al.*, Phys. Rev. Lett. **72**, 1415 (1994).
- [18] D. Beavis *et al.*, Phys. Rev. Lett. **75**, 3078 (1995).
- [19] A. Rusek *et al.*, Phys. Rev. C **54**, R15 (1996).
- [20] G. Applequist *et al.*, Phys. Rev. Lett. **76**, 3907 (1996).
- [21] P. Haridas *et al.*, Nucl. Instrum. Methods Phys. Res., Sect. A **385**, 412 (1997).
- [22] K. Barish, Ph.D. thesis, Yale University, 1996.
- [23] K. Barish *et al.*, Nucl. Instrum. Methods (to be published).
- [24] T. A. Armstrong *et al.* (to be published).

- 
- [25] K. Barish, for the E864 Collaboration, in *Proceedings of the Conference on Strangeness in Hadronic Matter, Budapest, 1996*, edited by T. Csörgö *et al.* (Akadémiai Kiadó, Budapest, 1996), p. 423.
- [26] F.S. Rotondo, for the E864 Collaboration, Nucl. Phys. **A610**, 297c (1996).
- [27] J.L. Nagle, Ph.D. thesis, Yale University, 1997.
- [28] S. Coe, Ph.D. thesis, Yale University, 1997.
- [29] J.K. Pope, for the E864 Collaboration, in *Proceedings of Heavy Ion Physics at the AGS (HIPAGS), Detroit, 1996*, edited by C.A. Pruneau *et al.* (Wayne State University Report No. WSU-NP-96-16, 1996), p. 119.